Polymer Journal (2015) 47, 267–277

www.nature.com/pj

ORIGINAL ARTICLE

Electrospinning of gelatin nanofiber scaffolds with mild neutral cosolvents for use in tissue engineering

Hiroyoshi Aoki, Hiromi Miyoshi and Yutaka Yamagata

Electrospun gelatin nanofibers are effective tissue engineering scaffolds with high biocompatibility and cell adhesion activity. In gelatin electrospinning, fluorinated alcohols, which are irritants, and acidic organic solvents are used as solvents to prevent gelation. This study established a technique to embed protein reagents into the nanofibers using mild solvents. From 22 mixtures of 50% organic solvent–50% H_2O, less denaturing neutral dipolar aprotic solvents (specifically *N*,*N*-dimethylacetamide, *N*,*N*-dimethylformamide and *N*-methyl-2-pyrrolidone), were screened to assess their suitability for use in electrospinning of gelatin nanofiber scaffolds by their ability to maintain gelatin in a sol state at room temperature. By selecting the solvents and their concentrations, gelatin nanofibers were electrospun with different structures from a thick, wide, porous nanofibrous structure to a thin, fine, nanofibrous mesh structure. Swiss 3T3 fibroblasts grew well on the gelatin nanofibers. In particular, some cells showed *in vivo*-like spindle morphologies on the thick porous nanofibers using *N*,*N*-dimethylacetamide. Additionally, as a model protein reagent, alkaline phosphatase was embedded in the gelatin nanofibers while maintaining high activity. Considering these results, the gelatin nanofibers in this study are expected to provide effective structural and chemical cues and will be useful for tissue engineering and regenerative medicine.
Polymer Journal (2015) **47,** 267–277; doi:10.1038/pj.2014.94; published online 19 November 2014

INTRODUCTION

In the field of regenerative medicine, one general strategy is to implant cells into tissue engineering scaffolds and then incorporate these into the patient's body.[1–4] The tissue engineering scaffolds must be made from biocompatible materials. Additionally, the scaffolds are required to provide mechanical support for transplanted cells until newly formed tissues are structurally stabilized. Furthermore, the scaffolds should be designed to regulate cellular processes, such as proliferation, differentiation and secretion of hormones and growth factors. Both structural and chemical cues provided by the extracellular matrix (ECM) are critical for tissue development with appropriate functions.[5,6] Electrospun nanofibers have been widely recognized as an excellent synthetic ECM that can provide mechanical support and structural cues to adherent cells.[7,8] Concerning the chemical cues, the nanofibers must be designed so that embedded protein reagents, such as growth factors and cytokines,[9] will be gradually released through degradation of the nanofibers *in vivo*.[10]

Electrospinning has been extensively studied to fabricate thin films,[11] highly precise electrostatic micropatterns,[12,13] and nanofibers.[7,8,14,15] In nanofiber electrospinning, a polymer solution is continuously supplied to a thin metallic needle by a pump.[7,8,15] The polymer solution is electrostatically sprayed from the needle tip by applying a high voltage. The electrospun polymer jet is further split into fine nanofibers through a Coulomb explosion. The nanofibers are immediately dried and deposited on a conductive substrate, forming a non-woven fabric. The electrospinning process can be controlled by many experimental conditions, such as the voltage, the polymer flow rate, the distance between the needle and the substrate, and the polymer solution.[7,8,15] The polymer solution conditions include the viscosity, surface tension, electric conductivity, polymer molecular weight and solvent volatility. Adjustment of these conditions enables control of the morphology of the fabricated nanofibrous structure.

Gelatin, which is solubilized from collagen in animals, has been actively studied to fabricate biocompatible nanofiber scaffolds for tissue engineering.[16–21] In electrospinning, gelatin is dissolved in solvents that allow it to be maintained in a sol state. These solvents include fluorinated alcohols[16,17] and acidic organic solvents.[18–21] The fluorinated alcohols (for example, 1,1,1,3,3,3-hexafluoro-2-propanol, denoted as HFP, and 2,2,2-trifluoroethanol) are volatile denaturing protein solubilizers.[22] Without a denaturant, heat-dissolved gelatin immediately forms gel at the needle tip at room temperature. The formation of this gelatin gel at the tip prevents it from being electrospun into nanofibers by the electrostatic force. Because the fluorinated alcohols highly denature gelatin to prevent gelation, the gelatin that is dissolved in the fluorinated alcohols can be easily electrospun into nanofibers.[16,17]

The gelatin nanofibers are also electrospun using acidic organic solvents (for example, acetic acid-ethyl acetate-H_2O[19,21] and formic acid-ethanol-H_2O[20]). Fluorinated alcohols and acidic organic solvents are appropriate solvents for fabricating a well-defined nanofibrous structure. Unfortunately, they have a tendency to denature protein reagents, such as growth factors and cytokines. Thus, to fabricate

Center for Advanced Photonics, RIKEN, Saitama, Japan
Correspondence: Dr H Aoki, Center for Advanced Photonics, RIKEN, 2-1 Hirosawa, Wako-shi, Saitama 351-0198, Japan.
E-mail: haoki@riken.jp
Received 2 March 2014; revised 26 August 2014; accepted 11 September 2014; published online 19 November 2014

nanofibers that provide chemical cues by diffusion and degradation of the nanofibers *in vivo*, a technique using less denaturing, neutral solvents compared with fluorinated alcohols and acidic organic solvents is desired.

Electrospinning while heating the gelatin sol in water is a safer alternative approach.[23] However, heating leads to denaturing of the protein reagents.[24–26] In addition, heating significantly affects the gelatin viscosity, which is a critical parameter determining the gelatin nanofiber morphology. Thus, precise heating control is important to fabricate a well-defined gelatin nanofibrous structure[23] that can provide adequate structural cues for controlling cellular processes.

In this study, we established a simple and sophisticated process to fabricate gelatin nanofibers that can effectively provide both structural and chemical cues. We screened gelatin nanofiber fabrication conditions with less denaturing, neutral pH solvents at room temperature. The structural parameters of the gelatin nanofibrous structure, specifically the nanofiber diameters and the pore size between the fibers, were controlled by the electrospinning solvent conditions. The conditions of gelatin nanofiber fabrication with neutral pH solvents at room temperature highly conserved the activity of the protein reagent embedded in the nanofibers.

EXPERIMENTAL PROCEDURE

Materials

Gelatin (from bovine bone, gel strength 210–250 g cm^{-2}), glycine, acetone, 1,3-butandiol, 1,2-dimethoxyethane, *N*,*N*-dimethylacetamide (DMA), 1,3-dimethyl-2-imidazolidinone (DMI), *N*,*N*-dimethylsulfoxide (DMSO), 1,4-dioxane, ethanol, 2-ethoxyethanol, glycerol, HFP, 2-methoxyethanol, *N*-methyl-2-pyrrolidone (NMP), sulfolane, tetrahydrofuran, *t*-butyl alcohol and pNPP (*p*-nitrophenyl phosphate) were obtained from Wako (Tokyo, Japan). Ethylene glycol, methanol and *N*,*N*-dimethylformamide (DMF) were purchased from Junsei Chemical Co., Ltd. (Tokyo, Japan). Triethyleneglycol, 1,5-pentanediol and 4% (w v^{-1}) osmium tetroxide were obtained from Tokyo Chemical Industry Co., Ltd. (Tokyo, Japan). Isopropanol (IPA) was purchased from Kokusan Chemical Co., Ltd. (Tokyo, Japan). Twenty-five percent (w v^{-1}) glutaraldehyde (GA) solution (Grade I, for electron microscopy), penicillin-streptomycin (100× concentration), alkaline phosphatase (ALP, from bovine intestinal mucosa) and a BCIP/NBT Liquid Substrate System were purchased from Sigma Aldrich (St Louis, MO, USA). The GA solution was stored at −20 °C until use. Minimum essential medium alpha and fetal bovine serum were obtained from Gibco (Grand Island, NY, USA). A LIVE/DEAD Viability/Cytotoxicity Kit was purchased from Life Technologies (Carlsbad, CA, USA).

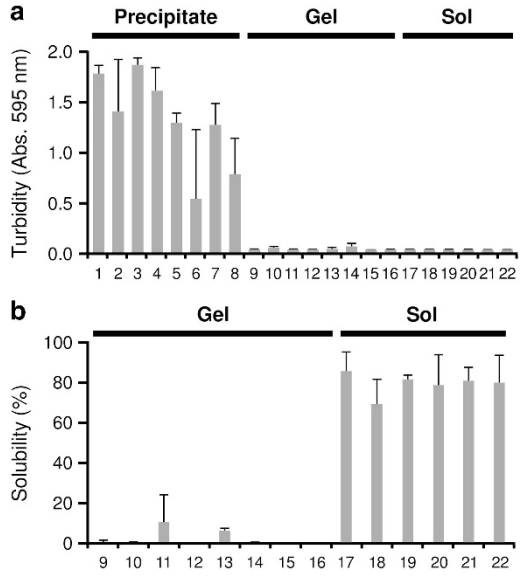

Figure 1 Screening of less denaturing polar neutral organic solvents for electrospinning of gelatin nanofibers. (**a**) Gelatin precipitates in 50% polar organic solvent–50% H_2O mixtures were quantified based on their turbidity at an absorbance of 595 nm ($n=3$). The polar organic solvents are indicated as follows. Precipitates: (1) acetone, (2) 1,2-dimethoxyethane, (3) 1,4-dioxane, (4) 2-ethoxyethanol, (5) tetrahydrofuran, (6) sulfolane, (7) isopropanol and (8) 1,5-pentanediol. Gels: (9) water (gel-state control), (10) methanol, (11) ethanol, (12) 1,3-butanediol, (13) 2-methoxyethanol, (14) ethylene glycol, (15) glycerol and (16) triethylene glycol. Sols: (17) HFP (sol-state control), (18) DMA, (19) DMF, (20) DMI, (21) DMSO and (22) NMP. (**b**) Gelatin gels and sols in 50% polar organic solvents were evaluated by their solubility in H_2O, as described in the Experimental procedure ($n=3$). A gelatin gel using H_2O and a heat-dissolved gelatin sol were used as gelatin gel (0% solubility) and sol (100% solubility) controls, respectively.

Screening of non-denaturing, neutral organic solvents for electrospinning of gelatin nanofibers

Water-miscible organic solvents were screened for their ability to maintain gelatin in a sol state. Gelatin was dissolved in water at a concentration of 20% (w v^{-1}) by autoclaving at 121 °C for 15 min and was then kept at 45 °C until mixing. After equal volumes of the gelatin solution and the polar organic solvents (Figure 1) were mixed in microtubes and left for 1 h at room temperature, the states of the mixtures were observed by the naked eye. The existence of the gelatin gels was confirmed by tilting the tubes and observing nonflowing meniscuses.[27]

The gelatin states in the 50% polar organic solvents were further quantified by their turbidity and solubility (Figure 1). The turbidity of the 10% (w v^{-1}) gelatin–50% (v v^{-1}) polar organic solvent–50% (v v^{-1}) H_2O in a 96-well microtiter plate (BD Falcon, Franklin Lakes, NJ, USA) was measured at 595 nm using a microplate reader (Model 550, Bio-Rad, Hercules, CA, USA) (Figure 1a). A gelatin-polar organic solvent mixture with absorbance at 595 nm of $\geqslant 0.5$ was defined as gelatin gel. The data in this study are presented as the mean ± s.d.

Gelatin gels or sols were further characterized by their solubility in H_2O. H_2O (1 ml) was added to 200 μl of the gelatin gel or sol in a microtube and, gently mixed by inverting. The solubility was assayed by the gelatin concentration in the supernatant with Coomassie Plus Protein Assay Reagent (Thermo Fisher Scientific Inc., Waltham, MA, USA). The solubility was calculated as $C_s/C_c \times 100$ (%), where C_s and C_c are the gelatin concentrations in the sample and the heat-dissolved gelatin sol control, respectively. Solubility values $<60\%$ and $\geqslant 60\%$ were defined as gels and sols, respectively. HFP and water were used as controls to form gelatin sol and gel states, respectively (Figure 1b).

The gelatin states were evaluated by the dielectric constants,[28] dipole moments[29–32] and Hansen solubility parameters (HSPs)[33–37] of the polar organic solvents. The HSP consists of polar (δ_p), hydrogen bonding (δ_h) and dispersion (δ_d) parameters. The HSP of a polar aprotic solvent-H_2O mixture (δ_{pm}, δ_{hm} and δ_{dm}) was calculated as follows:

$$\left(\delta_{pm},\ \delta_{hm},\ \delta_{dm}\right) = \frac{\left[\left(a\times\delta_{ps}+b\times\delta_{pw}\right),\left(a\times\delta_{hs}+b\times\delta_{hw}\right),\left(a\times\delta_{ds}+b\times\delta_{dw}\right)\right]}{100} \quad (1)$$

The HSPs of the polar organic solvent and H_2O are presented as (δ_{ps}, δ_{hs}, δ_{ds}) and (δ_{pw}, δ_{hw}, δ_{dw}), respectively.[36] The percentages (v v^{-1}) of the polar organic solvent and H_2O are shown as *a* and *b*. The collagen HSP[33] was used for estimating gelatin HSP (δ_{pg}, δ_{hg}, δ_{dg}). The HSP distance between gelatin and a solvent (R_a) was calculated as follows:

$$R_a = \sqrt{\left(\delta_{pg}-\delta_{ps}\right)^2+\left(\delta_{hg}-\delta_{hs}\right)^2+4\times\left(\delta_{dg}-\delta_{ds}\right)^2} \quad (2)$$

For the polar aprotic solvent-H_2O mixtures, (δ_{pm}, δ_{hm}, δ_{dm}) was used instead of (δ_{ps}, δ_{hs}, δ_{ds}).

Electrospinning of gelatin nanofibers using the dipolar aprotic solvents

Electrospinning of gelatin nanofibers was optimized using the dipolar aprotic solvents. Gelatin (5, 10 and 20%, w v^{-1}) was dissolved in the 50% organic

solvents–50% H_2O. The organic solvents used were DMA, DMF, DMI, DMSO, NMP and HFP. A syringe equipped with a 21G metal needle (Musashi Engineering, Inc., Tokyo, Japan) was filled with the gelatin solution containing the organic solvent in an electrospinning apparatus (model ES-2000, Fuence, Saitama, Japan).[38] The needle was placed above aluminum foil on a conductive collector, and the distance between the tip and the foil was approximately 130 mm. The gelatin solution was electrospun for 10 min, and the electrospun gelatin nanomaterials were electrostatically collected on the aluminum foil through a square hole (30 mm × 30 mm) in a Teflon mask. The Coulomb explosion plume was monitored based on its scattered light by illuminating it with a laser in the apparatus (Supplementary Figure S1). The electrostatic voltage (10–14 kV) and the pump speed (1–5 μl min^{-1}) were manually controlled to maintain the continuous plume and to prevent gelatin droplets from falling onto the aluminum foil (Supplementary Figure S1 and Supplementary Table S1). The electrospun gelatin deposits were sputter-coated with gold for 30 s three times, and their morphologies were observed using a scanning electron microscope (SEM, model VE-7800, Keyence Corporation, Osaka, Japan).

Effect of the concentration of the dipolar aprotic solvents on gelatin nanofiber electrospinning

The effects of the dipolar aprotic solvent concentration on the gelatin solubility and electrospinning were evaluated. After gelatin (0.8 g) was dissolved in 20–100% DMA, DMF and NMP solvents by autoclaving at 121 °C for 15 min, the gelatin solutions were filled with up to 20% (w v^{-1}) with the solvents. The gelatin solubility in the solvents was evaluated as described above. Because the boiling point (bp) of HFP is 58 °C, 20% gelatin in 20–100% HFP was dissolved at 50 °C overnight. The mixtures of dipolar aprotic solvent-H_2O showing greater than 60% gelatin solubility, which were 20–50% DMA, DMF, NMP and 20–100% HFP, were used for 20% gelatin electrospinning. The nanofiber morphologies were observed using SEM. The gelatin nanofiber diameters were measured based on the SEM images using ImageJ (US National Institute of Health, Bethesda, Maryland).[39]

Evaluation of the gelatin viscosities and morphologies of the crosslinked gelatin nanofibrous structure

The viscosities of 20% gelatin in the electrospinning solvents using 50% DMA, DMF, NMP and HFP were analyzed using a viscometer (model SV-1A, A & D Company, Tokyo, Japan) after 30 min at room temperature.

After the gelatin solutions were electrospun as described above, the gelatin nanofibers were insolubilized by chemical GA crosslinking,[40] and the crosslinked morphologies were evaluated. The gelatin nanofibers were cut into approximately 12-mm square pieces, after which they were crosslinked with 2.5% (w v^{-1}) GA-IPA at room temperature for 1 h and subsequently washed three times with IPA. The residual GA in the gelatin nanofibers was blocked by submerging them in 0.5 M glycine at room temperature for 1 h. Although GA is widely used in various fields, including as a crosslinker for biomedical materials, antigenicity deactivation of heart valves, and sterilization of medical devices, free GA is highly cytotoxic.[40] Therefore, GA was completely removed from the crosslinked gelatin nanofibers by washing three times in phosphate-buffered saline for 2 h each. The crosslinked gelatin nanofibers were glued onto coverslips (No. 1, 18-mm square, Matsunami Glass Ind., Ltd., Osaka, Japan) using epoxy adhesive (Araldite Rapid, Huntsman Corporation, The Woodlands, TX, USA).

The crosslinked gelatin nanofibers were observed using a field-emission SEM (model JSM-6330F, JEOL Ltd., Tokyo, Japan) at the Materials Characterization Support Unit at the RIKEN Center for Emergent Matter Science. The nanofiber diameters and the pore sizes between the fibers were measured based on the SEM images using ImageJ. The experiment was repeated three times.

Culture of Swiss 3T3 fibroblasts on the gelatin nanofiber scaffolds

Swiss 3T3 fibroblasts (RIKEN BioResource Center, Tsukuba, Ibaraki, Japan) were used as a model cell line in this study. These fibroblasts were cultured on the crosslinked gelatin nanofiber scaffolds and their morphologies were analyzed. The top and bottom sides of the gelatin nanofiber scaffolds were sterilized in ϕ 35-mm plastic dishes with a UV lamp for 30 min each. The gelatin nanofiber scaffolds were immersed in minimum essential medium alpha supplemented with 10% fetal bovine serum and 1% penicillin-streptomycin. Swiss 3T3 fibroblasts were seeded onto the gelatin nanofiber scaffolds at a density of approximately 2.8×10^3 cell mm^{-2}. They were cultured in 5% CO_2 at 37 °C overnight. A plastic dish and a 20% gelatin-H_2O gel that was crosslinked with GA were used as control substrates. Cell viabilities on the gelatin nanofiber scaffolds were evaluated using the LIVE/DEAD Viability/Cytotoxicity Kit with the three substrates.

For SEM observation of the Swiss 3T3 cells on the crosslinked gelatin nanofiber scaffolds, the cells were sequentially subjected to 2.5% GA fixation, 2% (w v^{-1}) osmium tetroxide fixation, stepwise 25–100% ethanol drying, and *t*-butyl alcohol drying.[41] After Pt-Pd sputtering for 30 s, obliquely from the upper left- and right sides, the cells were observed using the field-emission SEM. The experiment was repeated three times.

Evaluation of protein activity in the gelatin nanofibers

Using ALP as a model protein, protein stabilities were evaluated in the gelatin-electrospinning solvents and the electrospun gelatin nanofibers after GA crosslinking.

First, ALP (1 mg ml^{-1} final concentration) was mixed with 20% gelatin in the 50% DMA–50% H_2O (pH 7.0), the 50% DMF–50% H_2O (pH 7.0), and the 50% NMP–50% H_2O (pH 7.0) solvents. Conventional electrospinning solvents, such as 50% HFP–50% H_2O (pH 5.0) and 48% acetic acid–32% ethyl acetate–20% H_2O (pH 1.0),[19] were also used as controls. After the mixtures were incubated at 37 °C for 10 min, they were diluted 10-fold in 50 mM Tris-HCl (pH 9.0). The residual ALP activities were colorimetrically detected using a pNPP assay as follows.[42]

Briefly, 200 μl of diluted ALP containing 2 mM pNPP-100 mM Tris-HCl (pH 9.0)-2 M NaCl was incubated at 37 °C for 10 min, and then the ALP reaction was stopped by adding 100 μl of 0.5 M NaOH. The resulting *p*-nitrophenol concentration was measured at an absorbance of 420 nm using a spectrometer (model V-530, JASCO, Tokyo, Japan) and the delta absorbance was obtained by subtracting absorbance of a blank. Residual activities of ALP in the gelatin-electrospinning solvents were calculated as $\Delta_s/\Delta_c \times 100$ (%), where Δ_s and Δ_c are the delta absorbances of the gelatin-electrospinning solvents and that of the water, respectively.

Second, the stability of ALP in the GA-crosslinked gelatin nanofibers was also assayed as follows. ALP-embedded gelatin nanofibers were fabricated by electrospinning 1 mg ml^{-1} of ALP–20% gelatin–50% DMA, DMF, HFP or NMP–50% H_2O according to the method described above. As described in the above section, the electrospun nanofibers were crosslinked with GA and then fixed on coverslips. The ALP activities in the gelatin nanofiber using NMP (negative control) and the ALP-embedded gelatin nanofibers were assayed at 37 °C for 10 min by submerging the nanofibers in a BCIP/NBT Liquid Substrate System. The ALP reactions were stopped by washing the nanofibers in water three times.

RESULTS

Dipolar aprotic solvents maintaining the gelatin-sol state at room temperature

Mixtures of neutral polar organic solvents and H_2O (50%:50%) were screened for their ability to maintain gelatin in a sol state during electrospinning. After heat dissolved, 20% (w v^{-1}) gelatin-H_2O was mixed with an equal volume of the polar aprotic solvents, gelatin was precipitated, gelatinized or maintained in a sol state by the solvents at room temperature. Hydrophobic polar organic solvents (acetone, ethers and some hydrophobic alcohols) precipitated gelatin (Figure 1a), whereas hydrophilic protic solvents (water, some hydrophilic alcohols, glycols and glycerol) formed gelatin gels (Figure 1b). Interestingly, a gelatin sol was maintained by some dipolar aprotic solvents, specifically, DMA, DMF, DMI, DMSO and NMP, as well as the HFP gelatin sol-state control (Figure 1b).

Because the intermolecular hydrogen bonds of gelatin contribute to the formation of a gel,[43,44] the polarities of the organic solvents are

important for the gelatin states in the solvents. Therefore, the gelatin states in the organic solvent-H_2O mixtures were compared according to the dielectric constants[28] and dipole moments[29–32] of the organic solvents, which are representative polar parameters (Figure 2). The gelatin-precipitating solvents and the gelatin-gel-forming solvents are widely distributed in terms of having low and high levels of dielectric constants and dipole moments, respectively. Due to the carbonyl group, the dipolar aprotic solvents that allowed a gelatin-sol to form show high dielectric constants and dipole moments, which are narrowly distributed (approximately 38.9 and 3.93 D, respectively).

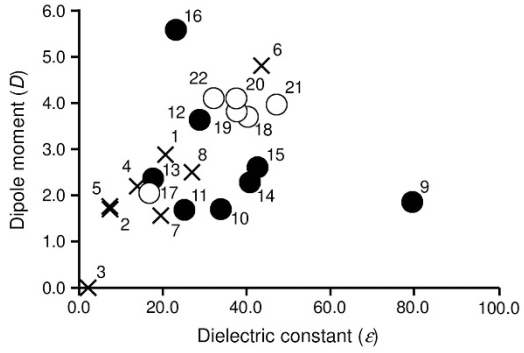

Figure 2 Relationship between the gelatin states in 50% polar organic solvent–50% H_2O mixtures and the organic solvent polarity. Dielectric constants (relative permittivity, ε) and dipole moments (D) in Debye units (1 D $=1.33564\times10^{-30}$ C m) of the polar organic solvents are plotted in Figure 1. Gelatin as a precipitate, a gel or a sol of gelatin is indicated by a cross, a filled circle, or an open circle, respectively. Solvent numbers are the same as in Figure 1.

The gelatin states in the organic solvent-H_2O mixtures were also evaluated based on the HSP.[33–37] The HSP represents a substance's solubility as polar (δ_p), hydrogen bonding (δ_h) and dispersion (δ_d) cohesion parameters. An HSP distance between two substances (R_a) represents their solubility similarity: low R_a suggests high solute solubility in a solvent. Notably, the R_a between 50% gelatin-sol-forming dipolar aprotic solvents and gelatin was lower than those of 50% gelatin-precipitating and gel-forming solvents (Table 1; Figure 3). These results suggest that hydrophilic dipolar aprotic cosolvents maintain gelatin in a sol state at room temperature, and the HSP would be useful for selecting cosolvents that maintain gelatin in the sol state.

Electrospinning of gelatin nanofibers using dipolar aprotic solvents

The gelatin nanofiber-forming properties of the screened dipolar aprotic solvents were investigated using HFP as a conventional control. Five percent (w v^{-1}) gelatin in the 50% dipolar aprotic solvents–50% H_2O was electrospun on aluminum foils. Electrospun deposits of 5% gelatin in 50% DMA, DMF, NMP and HFP–50% H_2O were very dry, and these electrospinning solvents completely vaporized during the electrospinning process (Figure 4a). In contrast, using 50%

Table 1 Hansen solubility parameters (HSPs) of gelatin and the polar organic solvents

		δ_p	δ_h	δ_d						*Ref.*
Gelatin		20.3	23.6	16.0						33
Gelatin state	*Polar organic solvent*	*50%*				*100%*				
		δ_p	δ_h	δ_d	R_a	δ_p	δ_h	δ_d	R_a	
Precipitate	Acetone	9.9	26.6	15.9	10.9	3.7	10.9	16.3	20.9	34
	1,2-Dimethoxyethane	11.0	24.2	15.5	9.4	6.0	6.0	15.4	22.7	35
	1,4-Dioxane	8.9	24.9	17.3	11.7	1.8	7.4	19.0	25.3	34
	2-Ethoxyethanol	12.6	28.3	15.9	9.0	9.2	14.3	16.2	14.5	35
	Isopropanol	11.1	29.4	15.7	10.9	6.1	16.4	15.8	15.9	34
	1,5-Pentanediol	14.1	32.6	14.7	11.2	12.2	22.8	13.9	9.2	36
	Sulfolane	16.3	24.9	17.0	4.6	16.6	7.4	18.4	17.3	34
	Tetrahydrofuran	10.9	25.2	16.2	9.6	5.7	8.0	16.8	21.4	34
Gel	Ethanol	12.4	30.9	15.7	10.7	8.8	19.4	15.8	12.2	34
	2-Methoxyethanol	12.6	29.4	15.9	9.6	9.2	16.4	16.2	13.2	35
	1,3-Butanediol	13.0	31.9	16.1	11.1	10.0	21.5	16.6	10.6	34
	Ethylene glycol	13.5	34.2	16.3	12.6	11.0	26.0	17.0	9.8	34
	Glycerol	14.1	35.8	16.5	13.7	12.1	29.3	17.4	10.4	34
	H_2O	16.0	42.3	15.5	19.2	16.0	42.3	15.5	19.2	34
	Methanol	14.2	32.3	15.3	10.7	12.3	22.3	15.1	8.3	34
	Triethylene glycol	14.3	30.5	15.8	9.2	12.5	18.6	16.0	9.3	34
Sol	*N,N*-Dimethylacetamide (DMA)	13.8	26.3	16.2	7.1	11.5	10.2	16.8	16.1	34
	N,N-Dimethylformamide (DMF)	14.9	26.8	16.5	6.4	13.7	11.3	17.4	14.2	34
	1,3-Dimethyl-2-imidazolidinone (DMI)	13.3	26.0	16.8	7.6	10.5	9.7	18.0	17.5	37
	N,N-Dimethylsulfoxide (DMSO)	16.2	26.3	17.0	5.2	16.4	10.2	18.4	14.8	34
	1,1,1,3,3,3-Hexafluoro-2-propanol (HFP)	10.2	28.5	16.4	11.3	4.3	14.7	17.2	18.5	34
	N-Methyl-2-pyrrolidone (NMP)	14.2	24.8	16.8	6.4	12.3	7.2	18.0	18.7	34

The HSP of polar (δ_p), hydrogen bonding (δ_h) and dispersion (δ_d) parameters ($MPa^{1/2}$) is shown. The HSP of the polar organic solvents evaluated in Figure 1 is indicated as 50% concentration–50% H_2O mixtures and 100% concentrations. R_a values ($MPa^{1/2}$) are the HSP distances between gelatin and the polar organic solvents, as described in the Experimental procedure. Lower R_a suggests higher gelatin solubility in the solvent.

DMSO–50% H_2O and 50% DMI–50% H_2O, the deposited gelatin was wet and did not form nanofibrous structure (data not shown).

Solvents containing 5, 10 and 20% (w v^{-1}) gelatin mixtures were electrospun, and their morphologies were evaluated. In previous reports, the electrospun polymer morphologies changed from nanoparticles to beads and threads, and then to nanofibers by increasing the polymer concentration and viscosity.[7,15] Consistent with these previous findings, 5, 10 and 20% gelatin solutions were deposited as nano- or micro-particles, beads and threads, and nanofibers, respectively (Figure 4b). In the following experiments, 20% gelatin was used for electrospinning. The gelatin nanofibers using DMA, DMF, NMP and HFP were named GNF-DMA, GNF-DMF, GNF-NMP and GNF-HFP, respectively.

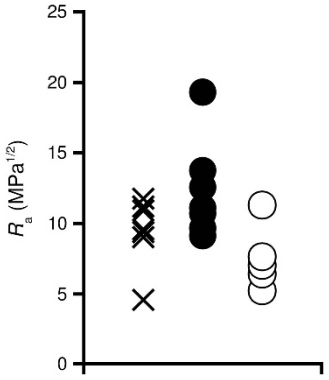

Figure 3 Relative gelatin solubility estimated by the HSP in the precipitating, gel-forming and sol-allowing solvents. The R_a values between gelatin and the precipitating, gel-forming and sol-allowing solvents are plotted for the 50% polar organic solvents. The symbols are the same as in Figure 2.

Effects of dipolar aprotic solvent concentrations on gelatin solubility, electrospinning and nanofiber morphology

DMA, DMF, NMP and HFP concentrations were evaluated for electrospinning of gelatin nanofibers. Before electrospinning, the gelatin solubility was assayed in 20–100% polar organic solvent-H_2O mixtures. Twenty percent gelatin was completely dissolved in 20–40% DMA, DMF and NMP, as well as in 20–80% HFP (Figure 5a).

Polar organic solvent-H_2O mixtures, which were 20–50% DMA, DMF and NMP, as well as 20–100% HFP, were investigated in terms of whether gelatin in the solvents was electrospun into nanofibers. Gelatin in 20–50% DMA, DMF and NMP-H_2O was electrospun into nanofibers, although gelatin in 20% DMA and DMF showed bead-and-thread morphologies to a small extent (Figure 5b). Reductions of the polar aprotic solvents thinned the nanofibers (Figures 5b and c). Although 20 and 100% HFP caused gelatin nanoparticles and clogging of the needle tip due to the highly viscous gelatin, respectively, 40–80% HFP was able to electrospin gelatin nanofibers. In the following experiments, 50% DMA, DMF, NMP and HFP–50% H_2O were selected for gelatin electrospinning.

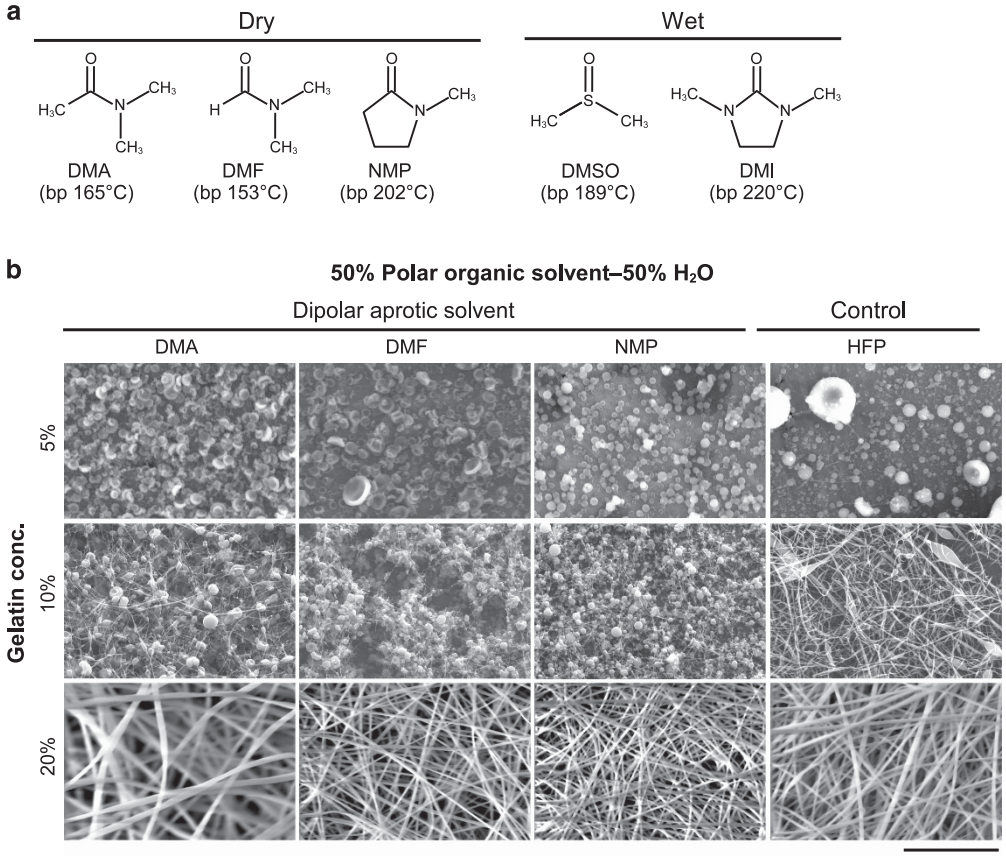

Figure 4 Morphologies of electrospun gelatin nanomaterials fabricated using screened dipolar aprotic solvents. (**a**) Chemical structures and bp of the solvents that allowed gelatin in a sol state to form. Whether the deposit was dry or wet is indicated at the top. (**b**) SEM images of electrospun gelatin nanomaterials formed by using different gelatin concentrations (5, 10 and 20%, w v^{-1}) in 50% organic solvents–50% H_2O. All of the images are shown at the same magnification. Bar: 10 μm.

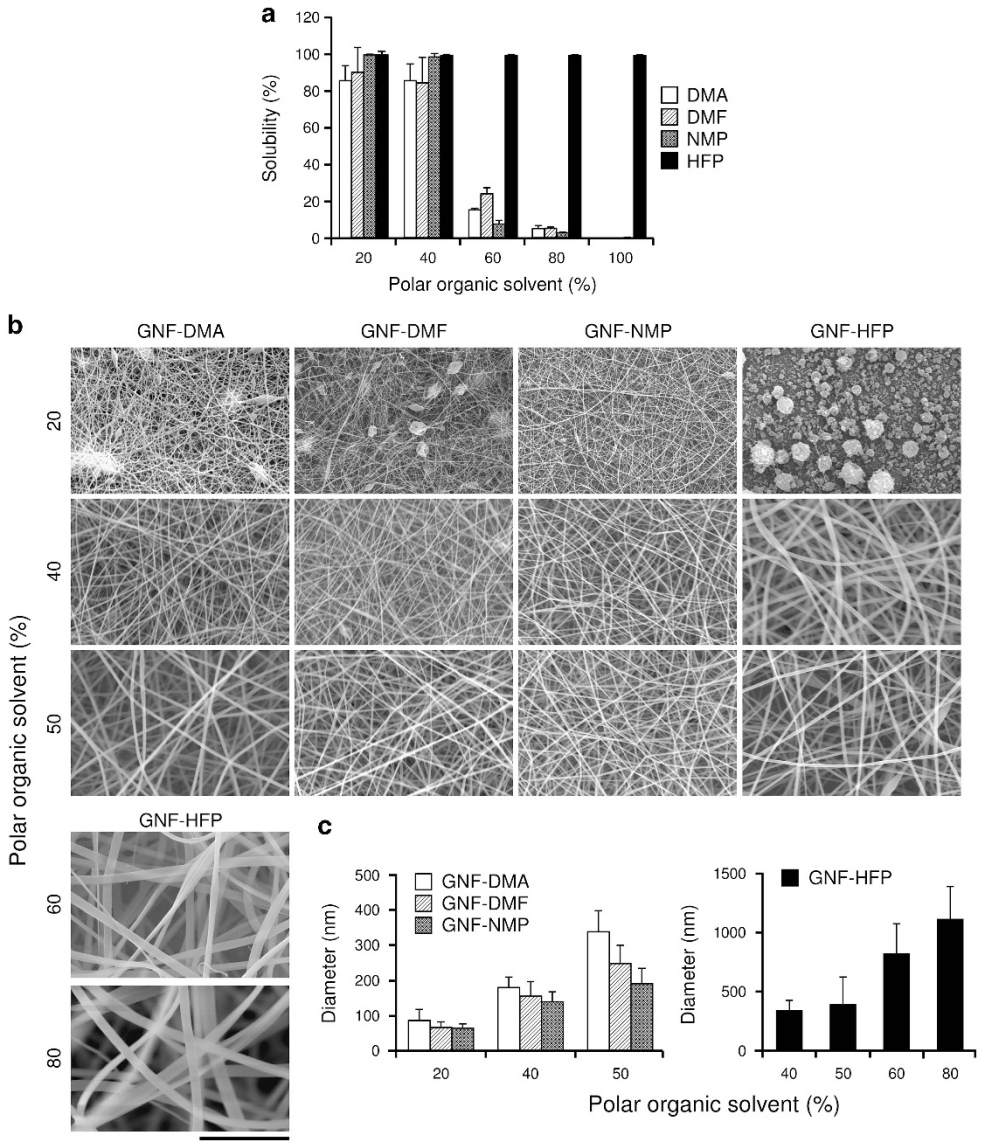

Figure 5 Effects of the concentration of dipolar aprotic solvents in gelatin nanofiber electrospinning. (**a**) Gelatin solubility in 20–100% DMA, DMF, NMP and HFP-H_2O. The gelatin solubility was assayed as in Figure 1b ($n = 3$). (**b**) Electrospun gelatin nanofibers with different concentrations of DMA, DMF, NMP and HFP. Gelatin nanofibers using DMA, DMF, NMP and HFP are termed GNF-DMA, GNF-DMF, GNF-NMP and GNF-HFP, respectively. All of the images are shown at the same magnification. Bar: 10 μm. (**c**) The diameters of the gelatin nanofibers in (**b**) are presented ($n = 50$).

Morphological control of the crosslinked gelatin nanofibrous structure by the selection of dipolar aprotic solvents

The water-soluble gelatin nanofibers were insolubilized by GA crosslinking for cell culture. Because the morphologies of crosslinked gelatin nanofibers would affect cell growth,[8] the fiber diameters and the scaffold pore sizes of the GA-crosslinked gelatin nanofibers were analyzed. The nanofibrous structures of GNF-DMA, GNF-DMF and GNF-NMP were well maintained after GA crosslinking, although GNF-HFP shrunk in the hydrophobic GA-IPA (Figure 6a). The fiber diameters of the GA-crosslinked gelatin nanofibers using the dipolar aprotic solvents increased in the order of GNF-DMA, GNF-DMF and GNF-NMP (Figure 6b).

Because polymer viscosity is reported to affect the nanofiber morphology,[7,15] the viscosities of the gelatin-electrospinning solvents were measured. The viscosities of the gelatin-electrospinning solvents were greater in the order of DMA > DMF > NMP > HFP. In the dipolar aprotic solvents, those with a higher dipole moment showed a lower gelatin viscosity (Figure 7a). The fiber diameter of the GA-crosslinked gelatin nanofibers using the dipolar aprotic solvents increased with the gelatin-electrospinning solvent viscosity (Figure 7b). Although the viscosity of 20% gelatin in the HFP electrospinning solvent was the lowest of the tested gelatin solutions, the diameter of GNF-HFP was thicker than those of GNF-DMF and GNF-NMP. Because HFP is more volatile (bp 58 °C) than the dipolar aprotic solvents (bp 153–202 °C, Figure 4a), the electrospun jets of the gelatin-HFP would rapidly dry before expanding into thinner nanofibers compared with the other nanofibers.

The porous structure of the gelatin nanofibers using the dipolar aprotic solvents was conserved after GA crosslinking. The pore size of the crosslinked gelatin nanofibrous structures using the dipolar aprotic solvents was in the order of GNF-DMA > GNF-DMF > GNF-NMP, as shown in Figures 6b and 7c. The pore size of the gelatin nanofibrous

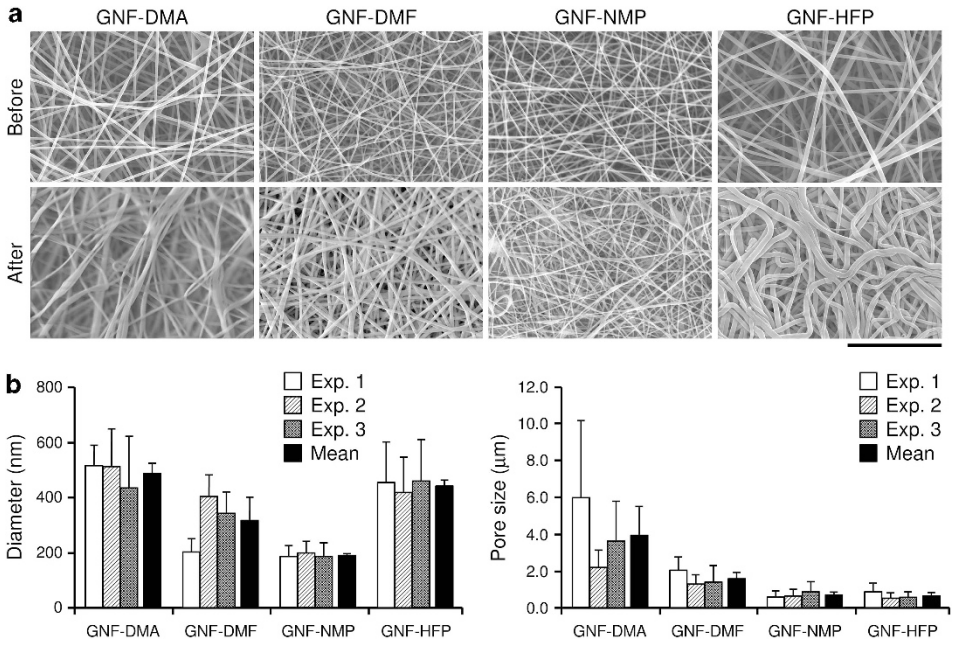

Figure 6 Gelatin nanofibers using the dipolar aprotic solvents maintained their nanofibrous porous structure after GA crosslinking. (**a**) Representative SEM images of gelatin nanofibers before and after GA crosslinking (experiment No. 3). All of the images are shown at the same magnification. Bar: 10 μm. (**b**) Fiber diameters (left panel) and pore sizes (right panel) of the gelatin nanofiber scaffolds after the GA crosslinking. The fiber diameters and the pore sizes of first, second and third experiments (Exp. 1–3) ($n = 50$, each) are indicated as open, diagonal and cross-hatched bars, respectively. The mean and standard deviation of the three experiments (mean, $n = 3$) are also represented as filled bars.

structure using the dipolar aprotic solvents positively correlated with the nanofiber diameter. Meanwhile, the GNF-HFP structure did not show this tendency due to vertical shrinking by aggregation on the aluminum foil in the hydrophobic GA-IPA solution. Thus, the nanofiber diameter and the pore size between the gelatin nanofibers fabricated with the dipolar aprotic solvents could be controlled based on the gelatin-sol viscosities, depending on the electrospinning solvents used.

Viabilities and morphologies of Swiss 3T3 fibroblasts in the gelatin nanofiber scaffolds

The gelatin nanofiber scaffolds of various diameters and pore sizes were evaluated in regard to their effects on cell viability and morphology. Swiss 3T3 fibroblasts grew well on the gelatin nanofiber scaffolds, as well as on the plastic dish and the GA-crosslinked gelatin gel control substrates (Figure 8; Table 2). The Swiss 3T3 fibroblasts showed a thin, flat morphology on the gelatin nanofibers. However, on the thick, porous GNF-DMA, some cells grew along the nanofibers with *in vivo*-like spindle shapes.[45] Considering these results, the nanofiber diameter and the pore size between the fibers affected the entire cell morphology of Swiss 3T3 fibroblasts.

Conservation of ALP activity in the gelatin nanofiber scaffolds using the dipolar aprotic solvents

Chemical, mechanical and structural cues are important for controlling cellular function and development.[5,6,46,47] To investigate the possibility that protein reagents, such as growth factors and cytokines, embedded into the gelatin nanofibers maintain their activities, the protein stabilities in the nanofibers using the neutral aprotic solvents were evaluated. ALP was used as a model reagent in this study because it can be quantitatively detected using a colorimetric method and is also used for bone tissue engineering.[48]

First, the ALP activities in the gelatin-electrospinning solvents were evaluated. Conventional electrospinning solvents, which were 50% HFP and 48% acetic acid-32% ethyl acetate, reduced the ALP activities to only $5 \pm 2\%$ and $2 \pm 1\%$, respectively (Figure 9). However, 50% DMA, DMF and NMP drastically conserved the ALP activities to levels of $100 \pm 0\%$, $94 \pm 10\%$ and $100 \pm 0\%$, respectively.

Next, ALP-embedded gelatin nanofibers were fabricated, and their ALP activities were compared. The ALP-embedded GNF-DMA, GNF-DMF and GNF-NMP showed high ALP activities, whereas the ALP-embedded GNF-HFP clearly showed less ALP activity (Figure 10). This result also indicates that the ALP activity in the gelatin nanofibers was maintained even after electrospinning, drying and GA crosslinking in hydrophobic IPA. Thus, GNF-DMA, GNF-DMF and GNF-NMP would be effective for embedding protein reagents while maintaining their activities.

DISCUSSION

Mild neutral dipolar aprotic solvents, DMA, DMF and NMP, were found to allow a gelatin-sol state to form at room temperature (Figures 1 and 2). Gelatin forms a gel by establishing intermolecular hydrogen bonds; however, this gelation is inhibited by substances such as 1,3-benzenediol,[43] formamide[44] and ethanolamine[49] by their direct hydrogen bonding with gelatin. The dipolar aprotic solvents lack a hydrogen bond donor and have carbonyl groups as electronegative acceptors, which are associated with high dielectric constants and dipole moments (Figures 2 and 4a).[50,51] Interestingly, the higher dipole moment reduced the viscosity of gelatin (Figure 7a). Therefore, the carbonyl group of the dipolar aprotic solvents would allow a gelatin-sol state with the disruption of intermolecular hydrogen bonds by solvating the gelatin.

The molecular polarities of dipolar aprotic solvents are reflected in their HSP.[34] The carbonyl groups and the lack of a hydrogen bond convey a high δ_p and a low δ_h to the dipolar aprotic solvents,

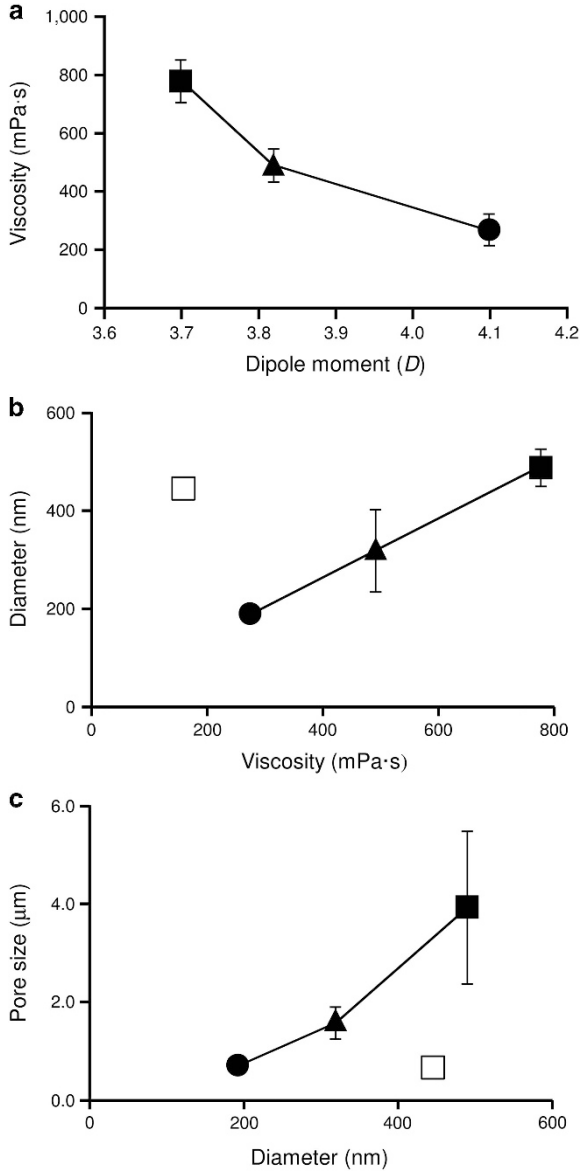

Figure 7 The gelatin viscosity in 50% dipolar aprotic solvent affected the gelatin nanofiber morphology. (**a**) The viscosities of the 20% (w v^{-1}) gelatin in the 50% dipolar aprotic solvents–50% H_2O are plotted against the dipole moments of the solvents. The scattered plots of (**b**) the diameters of GA-crosslinked gelatin nanofibers ($n=3$) and their mean viscosities and (**c**) the scaffold pore sizes ($n=3$) and their fiber mean diameters are also plotted. Filled rectangles, triangles and circles represent GNF-DMA, GNF-DMF and GNF-NMP, respectively. The open rectangle indicates GNF-HFP as a conventional control. The fiber diameters and the scaffold pore sizes of gelatin nanofibers are from Figure 6.

respectively (Table 1). As a result, the dipolar aprotic solvents were calculated to have lower R_a values than gelatin-precipitating and gel-forming solvents at 50% in H_2O (Figure 3). Thus, the HSP will be useful to screen electrospinning solvents that allow the formation of a gelatin-sol state.

Through electrospinning optimization, the screened DMA, DMF and NMP enabled the fabrication of gelatin nanofibers (Figure 4). DMA and DMF are milder than HFP, which is an irritant, although their toxicities are higher than that of NMP (Supplementary Table S2).[52,53] Thus, DMA and DMF were dried from the electrospun gelatin jets by traveling through air. The residual DMA and DMF in the gelatin nanofibers were desalted in phosphate-buffered saline after GA crosslinking. Because NMP has a low toxicity given its biodegradability (Supplementary Table S2) and high solubility for both hydrophilic and hydrophobic drugs, it has been used in clinical applications.[54–56] Therefore, GNF-NMP will be particularly appropriate for safe drug delivery. Thus, DMA, DMF and NMP will be safer electrospinning solvents than conventional HFP.

The diameter and pore size between fibers of the gelatin nanofibers using the dipolar aprotic solvents were controlled by appropriate selection of the solvent and its concentration (Figures 4b–7). In the Coulomb explosion, the fine splitting of the highly viscous polymer jet by the electrostatic repulsive force is difficult.[7,8,15] Therefore, the diameter of the gelatin nanofiber using the dipolar aprotic solvents had a positive correlation with the gelatin viscosity in the electrospinning solvent (Figure 7b).

The pore sizes of the gelatin nanofiber scaffolds were closely correlated with their fiber diameters (Figure 7c). Because the same amount gelatin was deposited, the number of thick gelatin nanofibers was less than that of thin nanofibers; therefore, the pore size increased with the fiber diameter. However, the porosity of GNF-HFP was reduced upon shrinking of the scaffold by nanofiber aggregation in the hydrophobic GA-IPA, whereas the porosities of the gelatin nanofibers using the dipolar aprotic solvents were preserved (Figure 6a). The less denaturing dipolar aprotic solvent would partially form gel in the nanofiber after electrospinning, which would strengthen the nanofibers against shrinking. However, the fiber strength of GNF-HFP would be weak due to the prevention of gel formation by the HFP denaturant. Therefore, the electrospinning cosolvents may affect the strength and the porosity change of the nanofiber after GA crosslinking. Thus, the porous structures of gelatin nanofibers using the dipolar aprotic solvents demonstrated the positive correlation between the fiber diameters and the pore sizes (Figure 7c).

The structural parameters of the gelatin nanofiber scaffolds affected the morphologies of Swiss 3T3 fibroblasts (Figure 8). The fiber diameter and porosity of the ECM affects the cell function and fate.[57] For example, the differentiation, morphology and growth of neural stem/progenitor cells are affected by the nanofiber diameter.[58] Swiss 3T3 fibroblasts showed flat shapes on the fine nanofibrous structures (GNF-DMF, GNF-NMP and GNF-HFP), and some cells grew along with the thick sparse gelatin nanofibers (GNF-DMA) with *in vivo*-like spindle morphology.[45] Thus, the fiber diameters and the pore sizes of the gelatin nanofiber scaffolds would affect the Swiss 3T3 fibroblast morphology. In ECM, collagen fibrils, which provide physical strength and act as a cell growth scaffold, were shown to have various diameters from several tens to several hundreds of nanometers in the human body.[59–61] Because the diameter of gelatin nanofibers using the dipolar aprotic solvents was controlled from 66 nm (GNF-NMP using 20% NMP) to 488 nm (GNF-DMA using 50% DMA) by selecting the solvent conditions (Figures 5–7), the gelatin nanofiber scaffolds using the dipolar aprotic solvents will be excellent to provide structural cues closely mimicking an *in vivo* ECM structure of target cells in regenerative medicine.

As a model protein, ALP was embedded in the gelatin nanofibers using the dipolar aprotic solvents with high activity (Figures 9 and 10). For drug delivery with nanofibers, protein reagents mixed in electrospun polymer are superior in terms of long-term release.[62] However, protein reagents are denatured by hydrophobic synthetic polymers and nonpolar organic solvents. Because gelatin and the 50% dipolar aprotic solvent–50% H_2O mixtures are hydrophilic, they maintain the activities of protein reagents embedded in the nanofibers. Because

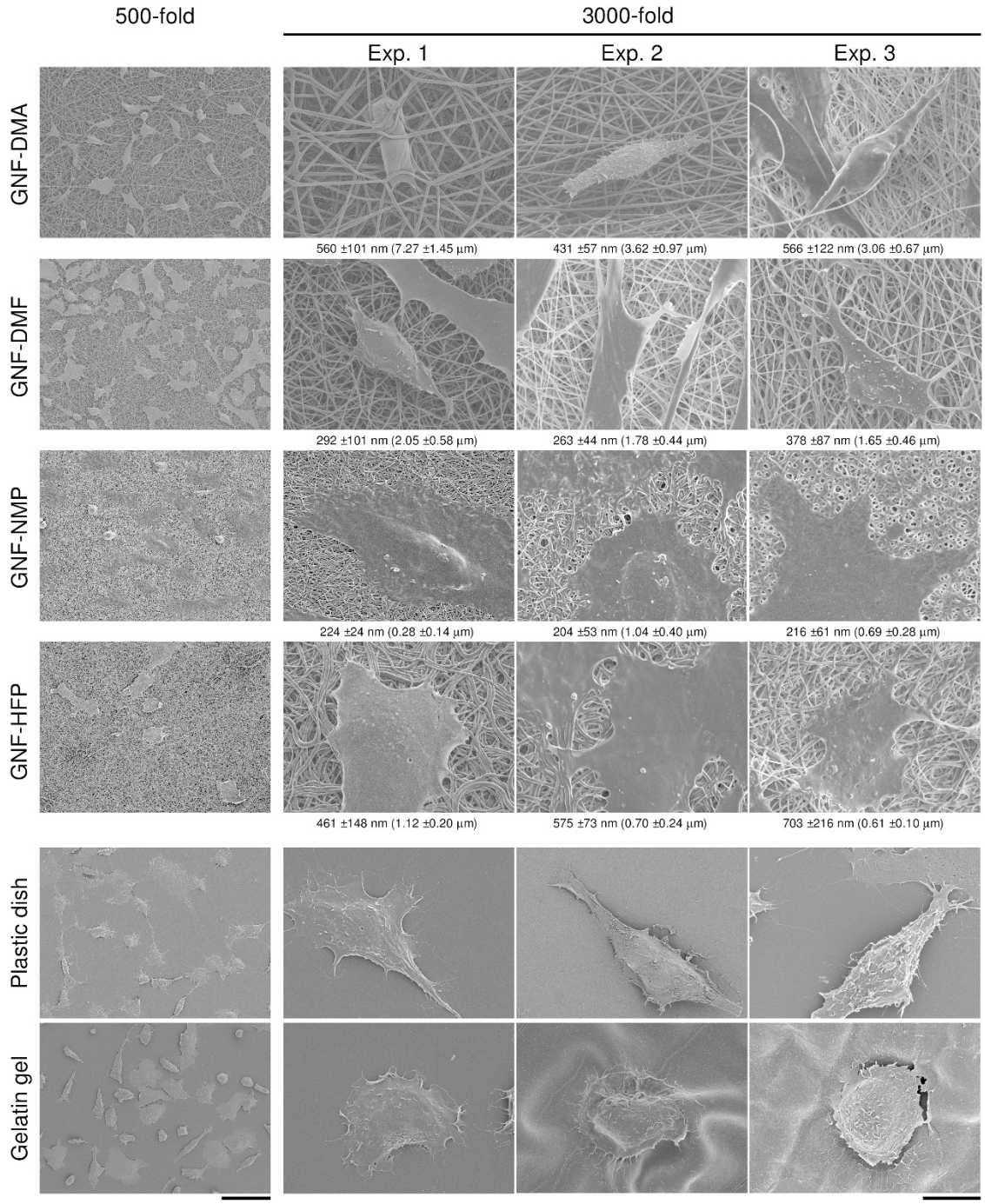

Figure 8 Swiss 3T3 fibroblasts on the gelatin nanofiber scaffolds. Swiss 3T3 fibroblast cells grown on GNF-DMA, GNF-DMF GNF-NMP, and conventional GNF-HFP were observed using SEM at 500- (Exp. 1) and 3000-fold magnifications (Exp. 1–3). Representative images at each magnification are shown at the same scale. Bars in the 500- and 3000-fold magnifications represent 50 and 5 μm, respectively. The plastic dish and the gelatin gel were used as the conventional control substrates. The diameters of the gelatin nanofibers in close contact with the Swiss 3T3 fibroblast cells are shown below each image ($n=10$). The scaffold pore sizes close to the cells are shown in parentheses ($n=5$).

the nanofiber scaffolds have high permeability,[7,8] the ALP-embedded nanofiber would enhance the enzyme reaction by diffusion through the substrate (Figure 10). The high permeability of the gelatin nanofiber scaffolds will also be effective for releasing embedded protein reagents from the nanofibers for drug delivery. Thus, the electrospinning solvents using the dipolar aprotic solvents are considered to be suitable for the fabrication of active growth factor-embedded gelatin nanofibers.

CONCLUSION

This study demonstrates a simple and sophisticated strategy to fabricate gelatin nanofiber scaffolds to provide well-defined structural

Table 2 Cell viabilities on the gelatin nanofiber scaffolds

Substrate	*Viability (%)*
GNF-DMA	99.3 ± 0.3
GNF-DMF	99.0 ± 0.2
GNF-NMP	99.4 ± 0.1
GNF-HFP	99.1 ± 0.2
Plastic dish	99.8 ± 0.2
Gelatin gel	98.8 ± 0.9

Abbreviations: GNF, gelatin nanofiber; DMA, *N*,*N*-dimethylacetamide; DMF, *N*,*N*-dimethylformamide; HFP, 1,1,1,3,3,3-hexafluoro-2-propanol; NMP, *N*-methyl-2-pyrrolidone. The cell viabilities ($n=3$) of Swiss 3T3 fibroblasts on the gelatin nanofiber scaffolds were evaluated using a LIVE/DEAD Viability/Cytotoxicity Kit, as described in the Experimental procedure. Control substrates, a plastic dish and a gelatin gel, are also indicated.

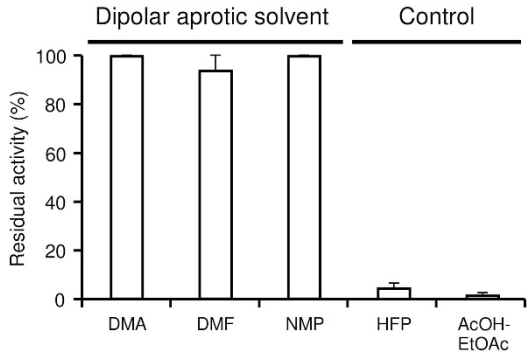

Figure 9 The electrospinning solvents using the dipolar aprotic solvents provided less denaturing conditions than conventional solvents. The protein stabilities, which were calculated as residual activities, in the 20% gelatin-electrospinning solvents were evaluated using ALP as a model. DMA, DMF, NMP and HFP represent 50% of each organic solvent–50% H_2O. AcOH-EtOAc is 48% acetic acid-32% ethyl acetate-20% H_2O, which is a conventional electrospinning solvent.

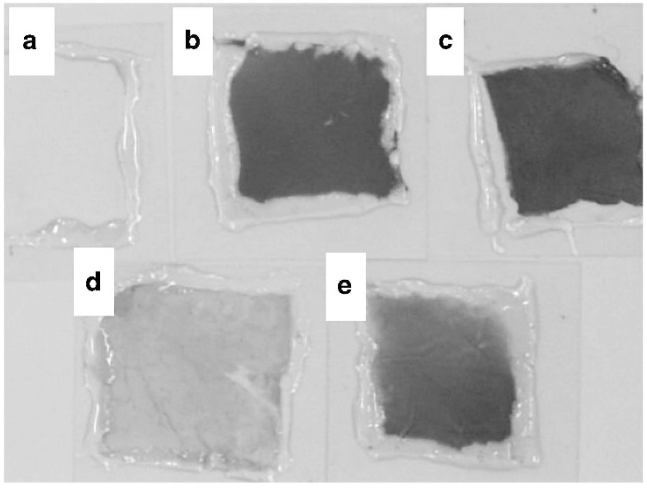

Figure 10 High ALP activities in gelatin nanofiber scaffolds fabricated with neutral dipolar aprotic solvents. The ALP activities in the GA-crosslinked gelatin nanofiber scaffolds were investigated using a colorimetric assay. Blue color indicates high ALP activity in the gelatin nanofibers. (**a**) GNF-NMP (negative control) and ALP-embedded gelatin nanofiber scaffolds of (**b**) GNF-DMA, (**c**) GNF-DMF, (**d**) GNF-HFP and (**e**) GNF-NMP. Bar: 10 mm.

cues and sustained delivery of chemical cues that are critical for tissue engineering. In our strategy, gelatin nanofibers were electrospun using less toxic, less denaturing, neutral dipolar aprotic solvents, namely, DMA, DMF and NMP. We clarified that two important structural parameters, the nanofiber diameter and the pore size between the fibers, can be designed by selecting an adequate solvent based on the viscosity of the gelatin solution used for electrospinning. Furthermore, the dipolar aprotic solvents conserved the activity of an embedded protein reagent in the nanofibers. In conclusion, the gelatin nanofiber scaffolds fabricated using these neutral dipolar aprotic solvents can be used for sustained delivery of a protein reagent by providing chemical cues concomitantly with physical cues. Therefore, these scaffolds will be useful in regenerative medicine.

ACKNOWLEDGEMENTS

This work was supported by JSPS KAKENHI Grant Number 23510139 and RIKEN. We thank Mr D Inoue at the Materials Characterization Support Unit at the RIKEN Center for Emergent Matter Science for his technical SEM support.

1 Takahashi, K., Yamanaka, S. Induction of pluripotent stem cells from mouse embryonic and adult fibroblast cultures by defined factors. *Cell* **126**, 663–676 (2006).
2 Evans, M. J., Kaufman, M. H. Establishment in culture of pluripotential cells from mouse embryos. *Nature* **292**, 154–156 (1981).
3 Robinton, D. A., Daley, G. Q. The promise of induced pluripotent stem cells in research and therapy. *Nature* **481**, 295–305 (2012).
4 Langer, R., Vacanti, J. P. Tissue engineering. *Science* **260**, 920–926 (1993).
5 Lu, P., Weaver, V. M., Werb, Z. The extracellular matrix: a dynamic niche in cancer progression. *J. Cell Biol.* **196**, 395–406 (2012).
6 Bukoreshtliev, N. V., Haase, K., Pelling, A. E. Mechanical cues in cellular signalling and communication. *Cell Tissue Res.* **352**, 77–94 (2013).
7 Sill, T. J., von Recum, H. A. Electrospinning: applications in drug delivery and tissue engineering. *Biomaterials* **29**, 1989–2006 (2008).
8 Kai, D., Jin, G., Prabhakaran, M. P., Ramakrishna, S. Electrospun synthetic and natural nanofibers for regenerative medicine and stem cells. *Biotechnol. J.* **8**, 59–72 (2013).
9 Discher, D. E., Mooney, D. J., Zandstra, P. W. Growth factors, matrices, and forces combine and control stem cells. *Science* **324**, 1673–1677 (2009).
10 Schneider, A., Wang, X. Y., Kaplan, D. L., Garlick, J. A., Egles, C. Biofunctionalized electrospun silk mats as a topical bioactive dressing for accelerated wound healing. *Acta Biomater.* **5**, 2570–2578 (2009).
11 Ju, J., Yamagata, Y., Higuchi, T. Thin-film fabrication method for organic light-emitting diodes using electrospray deposition. *Adv. Mater.* **21**, 4343–4347 (2009).
12 Kim, J. W., Yamagata, Y., Kim, B. J., Higuchi, T. Direct and dry micro-patterning of nano-particles by electrospray deposition through a micro-stencil mask. *J. Micromech. Microeng.* **19**, 025021–025029 (2009).
13 Aoki, H., Kaneko, A., Kajita, A., Yamagata, Y., Ike, F., Kase, H. An on-site serology monitoring system for laboratory mice using a multiplex microfluidic chip fabricated by the electrospray deposition method. *J. Chem. Eng. Jpn* **45**, 528–538 (2012).
14 Seo, H., Matsumoto, H., Hara, S., Minagawa, M., Tanioka, A., Yako, H., Yamagata, Y., Inoue, K. Preparation of polysaccharide nanofiber fabrics by electrospray deposition: additive effects of poly (ethylene oxide). *Polym. J.* **37**, 391–398 (2005).
15 Morota, K., Matsumoto, H., Mizukoshi, T., Konosu, Y., Minagawa, M., Tanioka, A., Yamagata, Y., Inoue, K. Poly(ethylene oxide) thin films produced by electrospray deposition: morphology control and additive effects of alcohols on nanostructure. *J. Colloid Interface Sci.* **279**, 484–492 (2004).
16 Zhang, Y., Ouyang, H., Lim, C. T., Ramakrishna, S., Huang, Z. M. Electrospinning of gelatin fibers and gelatin/PCL composite fibrous scaffolds. *J. Biomed. Mater. Res. B Appl. Biomater.* **72**, 156–165 (2005).
17 Tsai, S. W., Liou, H. M., Lin, C. J., Kuo, K. L., Hung, Y. S., Weng, R. C., Hsu, F. Y. MG63 osteoblast-like cells exhibit different behavior when grown on electrospun collagen matrix versus electrospun gelatin matrix. *PLoS ONE* **7**, e31200 (2012).
18 Choktaweesap, N., Arayanarakul, K., Aht-ong, D., Meechaisue, C., Supaphol, P. Electrospun gelatin fibers: effect of solvent system on morphology and fiber diameters. *Polym. J.* **39**, 622–631 (2007).
19 Song, J. H., Kim, H. E., Kim, H. W. Production of electrospun gelatin nanofiber by water-based co-solvent approach. *J. Mater. Sci. Mater. Med.* **19**, 95–102 (2008).
20 Chen, H. C., Jao, W. C., Yang, M. C. Characterization of gelatin nanofibers electrospun using ethanol/formic acid/water as a solvent. *Polymers Adv. Technol.* **20**, 98–103 (2009).
21 Angarano, M., Schulz, S., Fabritius, M., Vogt, R., Steinberg, T., Tomakidi, P., Friedrich, C., Mülhaupt, R. Layered gradient nonwovens of in situ crosslinked electrospun collagenous nanofibers used as modular scaffold systems for soft tissue regeneration. *Adv. Funct. Mater.* doi:10.1002/adfm.201202816 (2013).

22 Zeugolis, D. I., Khew, S. T., Yew, E. S. Y., Ekaputra, A. K., Tong, Y. W., Yung, L. Y. L., Hutmacher, D. W., Sheppard, C., Raghunath, M. Electro-spinning of pure collagen nano-fibres – Just an expensive way to make gelatin? *Biomaterials* **29**, 2293–2305 (2008).
23 Zhang, S., Huang, Y., Yang, X., Mei, F., Ma, Q., Chen, G., Ryu, S., Deng, X. Gelatin nanofibrous membrane fabricated by electrospinning of aqueous gelatin solution for guided tissue regeneration. *J. Biomed. Mater. Res. A* **90**, 671–679 (2009).
24 Westall, F. C., Rubin, R., Gospodarowicz, D. Brain-derived fibroblast growth factor: a study of its inactivation. *Life Sci.* **33**, 2425–2429 (1983).
25 Edelman, E. R., Mathiowitz, E., Langer, R., Klagsbrun, M. Controlled and modulated release of basic fibroblast growth factor. *Biomaterials* **12**, 619–626 (1991).
26 Santana, H., Gonzalez, Y., Campana, P. T., Noda, J., Amarantes, O., Itri, R., Beldarrain, A., Paez, R. Screening for stability and compatibility conditions of recombinant human epidermal growth factor for parenteral formulation: effect of pH, buffers, and excipients. *Int. J. Pharm.* **452**, 52–62 (2013).
27 Sanwlani, S., Kumar, P., Bohidar, H. B. Hydration of gelatin molecules in glycerol-water solvent and phase diagram of gelatin organogels. *J. Phys. Chem. B* **115**, 7332–7340 (2011).
28 Landolt-Börnstein Database, Springer Materials. http://www.springermaterials.com. Accessed 25 July 2013.
29 Lo, C. C., Chao, P. M. Replacement of carcinogenic solvent HMPA by DMI in insect sex pheromone synthesis. *J. Chem. Ecol.* **16**, 3245–3253 (1990).
30 Lide, D. R. (ed.) *Properties of Organic Solventss, ver.2.0* (CRC Press: Boca Raton, FL, USA, 1996).
31 Marcus, Y. *The Properties of Solvents* (Wiley: Chichester, UK, 1998).
32 Zhuravlev, V. I., Usacheva, T. M., Lifanova, N. V., Vydrina, E. P. Dielectric properties of polyhydric alcohols: butanediols. *Russ. J. Gen. Chem.* **78**, 1189–1196 (2008).
33 Miller, R. G., Bowles, C. Q., Chappelow, C. C., Eick, J. D. Application of solubility parameter theory to dentin-bonding systems and adhesive strength correlations. *J. Biomed. Mater. Res.* **41**, 237–243 (1998).
34 Hansen, C. M. *Hansen Solubility Parameters: A User's Handbook* (CRC Press LLC: Boca Ranton, FL, 1999).
35 Williams, D. L., Kuklenz, K. D. A determination of the Hansen solubility parameters of hexanitrostilbene (HNS). *Propellants Explos. Pyrotech.* **34**, 452–457 (2009).
36 Barton, A. F. M. *Handbook of Solubility Parameters and Other Cohesion Parameters*, 2nd edn (CRC Press LLC: Boca Ranton, FL, 1991).
37 Choi, E. Y., Han, T. H., Hong, J., Kim, J. E., Lee, S. H., Kim, H. W., Kim, S. O. Noncovalent functionalization of graphene with end-functional polymers. *J. Mater. Chem.* **20**, 1907–1912 (2010).
38 Hayakawa, T., Yoshinari, M., Nitta, K., Inoue, K. Collagen nanofiber on titanium or partially stabilized zirconia by electrospray deposition. *J. Hard Tissue Biol.* **19**, 5–12 (2010).
39 Schneider, C. A., Rasband, W. S., Eliceiri, K. W. NIH Image to ImageJ: 25 years of image analysis. *Nat. Methods* **9**, 671–675 (2012).
40 Jayakrishnan, A., Jameela, S. R. Glutaraldehyde as a fixative in bioprostheses and drug delivery matrices. *Biomaterials* **17**, 471–484 (1996).
41 Passey, S., Pellegrin, S., Mellor, H. Scanning electron microscopy of cell surface morphology. *Curr. Protoc. Cell Biol.* Chapter 4: Unit 4.17 (2007).
42 Fernley, H. in *The Enzymes* 3rd edn Vol 4: ed Boyer P. D. pp. 417–447 (Academic Press: New York, NY, USA, 1971).
43 Wu, J., Chiu, S., Pearce, E. M., Kwei, T. K. Effects of phenolic compounds on gelation behavior of gelatin gels. *J. Polym. Sci. A Polym. Chem.* **39**, 224–231 (2001).
44 Miyawaki, O., Norimatsu, Y., Kumagai, H., Irimoto, Y., Kumagai, H., Sakurai, H. Effect of water potential on sol-gel transition and intermolecular interaction of gelatin near the transition temperature. *Biopolymers* **70**, 482–491 (2003).
45 Yamada, K. M., Cukierman, E. Modeling tissue morphogenesis and cancer in 3D. *Cell* **130**, 601–610 (2007).
46 Friedl, P., Alexander, S. Cancer invasion and the microenvironment: plasticity and reciprocity. *Cell* **147**, 992–1009 (2011).
47 Cohen, D. E., Melton, D. Turning straw into gold: directing cell fate for regenerative medicine. *Nat. Rev. Genet.* **12**, 243–252 (2011).
48 Gkioni, K., Leeuwenburgh, S. C., Douglas, T. E., Mikos, A. G., Jansen, J. A. Mineralization of hydrogels for bone regeneration. *Tissue Eng. B Rev.* **16**, 577–585 (2010).
49 Umberger, J. Q. Solution and gelation of gelatin as related to solvent structure. *Photogr. Sci. Eng.* **11**, 385–391 (1967).
50 Parker, A. J. The effects of solvation on the properties of anions in dipolar aprotic solvents. *Q. Rev. Chem. Soc.* **16**, 163–187 (1962).
51 Ewell, R. H., Harrison, J. M., Berg, L. Azeotropic distillation. *Ind. Eng. Chem.* **36**, 871–875 (1944).
52 ChemIDplus Advanced. US National Library of Medicine (2014). http://chem.sis.nlm.nih.gov/chemidplus/. Accessed 15 May 2014.
53 Halocarbon, Hexafluoroisopropanol (HFIP) MSDS (2015). http://www.halocarbon.com/. Accessed 15 May 2014.
54 Sanghvi, R., Narazaki, R., Machatha, S. G., Yalkowsky, S. H. Solubility improvement of drugs using *N*-methyl pyrrolidone. *AAPS Pharm. Sci. Tech.* **9**, 366–376 (2008).
55 Jouyban, A., Fakhree, M. A., Shayanfar, A. Review of pharmaceutical applications of *N*-methyl-2-pyrrolidone. *J. Pharm. Pharmaceut. Sci.* **13**, 524–535 (2010).
56 Ligocka, D., Lison, D., Haufroid, V. Contribution of CYP2E1 to *N*-methyl-2-pyrrolidone metabolism. *Arch. Toxicol.* **77**, 261–266 (2003).
57 Schwartz, M. A., Chen, C. S. Cell biology. Deconstructing dimensionality. *Science* **339**, 402–404 (2013).
58 Christopherson, G. T., Song, H., Mao, H. Q. The influence of fiber diameter of electrospun substrates on neural stem cell differentiation and proliferation. *Biomaterials* **30**, 556–564 (2009).
59 Luria, E. A., Owen, M. E., Friedenstein, A. J., Morris, J. F., Kuznetsow, S. A. Bone formation in organ cultures of bone marrow. *Cell Tissue Res.* **248**, 449–454 (1987).
60 Doughty, M. J. Assessment of collagen fibril spacing in relation to selected region of interest (ROI) on electron micrographs–application to the mammalian corneal stroma. *Microsc. Res. Tech.* **75**, 474–483 (2012).
61 Franchi, M., Trire, A., Quaranta, M., Orsini, E., Ottani, V. Collagen structure of tendon relates to function. *ScientificWorldJournal* **7**, 404–420 (2007).
62 Ji, W., Sun, Y., Yang, F., van, J. J., Fan, M., Chen, Z., Jansen, J. A. Bioactive electrospun scaffolds delivering growth factors and genes for tissue engineering applications. *Pharm. Res.* **28**, 1259–1272 (2011).

Supplementary Information accompanies the paper on Polymer Journal website (http://www.nature.com/pj)